PNAS RESEARCH ARTICLE | NEUROSCIENCE

A serotonergic circuit regulates aversive associative learning under mitochondrial stress in *C. elegans*

Yueh-Chen Chiang[a,b], Chien-Po Liao[a,b,1], and Chun-Liang Pan[a,b,2]

Edited by Piali Sengupta, Brandeis University, Waltham, MA; received August 23, 2021; accepted February 1, 2022 by Editorial Board Member Michael Rosbash

Physiological stress profoundly alters the internal states of the animals and could drive aversive learning, but signaling and circuit mechanisms underlying such behavioral plasticity remain incompletely understood. Here, we show that mitochondrial disruption in nonneural tissues of *Caenorhabditis elegans* induces learned aversion for nutritious bacterial food that displays features of long-term associative memory. Serotonin secreted from the modulatory NSM neuron acts through the SER-4 receptor in the RIB interneuron to drive bacterial avoidance, with NSM and RIB required for the establishment and retrieval for learned aversion, respectively. NSM serotonin synthesis increases early in the induction of systemic mitochondrial stress. Calcium imaging reveals altered RIB responses to bacterial cues in a fraction of stress-primed but not naïve animals. These findings uncover cellular circuits and neuromodulation that enable aversive learning under stress, and lay the foundation for future exploration of behavioral plasticity governed by internal state changes.

C. elegans | serotonin | aversive learning | mitochondria | stress

Internal states include core physiological functions, such as feeding, metabolic balance, and tissue integrity, which animals constantly monitor to achieve homeostasis. Internal states are critical influences on animal behavior, enabling adaptation and learning that optimize organismal fitness and chance of survival under environmental fluctuations (1). For example, starved nematodes are motivated to cross highly aversive osmotic barriers in search of food, whereas fed worms avoid such repulsive barriers (2). Disruption of cellular functions by infection or toxin ingestion is another powerful influence on animal behavior, inducing avoidance to sensory cues associated with the pathogens or toxins (3). Such aversive learning is pervasive in nature, consistent with its ecological importance. However, the molecular correlates of distinct internal states are largely obscure, and how neural circuits integrate information on internal states to drive appropriate behaviors remain incompletely understood.

Mammalian serotonergic neurons are highly diversified and project broadly to various brain regions (4). Serotonin is an important neuromodulator involved in behavioral and cognitive processes associated with reward and changes of the internal states (4, 5). In the nematode *Caenorhabditis elegans*, serotonin is implicated in behaviors that are heavily dependent on internal states, such as egg laying, pharyngeal pumping, locomotion, and foraging behaviors (6–11). Serotonin promotes a persistent foraging state known as dwelling/exploitation, during which the animals restrict their movements within a smaller area, in contrast to the roaming/exploration state governed by pigment dispersal factor (PDF) neuropeptide signaling (11). The switch between dwelling and roaming is critically dependent on the feeding status, suggesting that serotonergic signaling connects internal states to foraging behaviors. The *C. elegans* hermaphrodite has a much simpler serotonergic system than that of the mammals, with three pairs of sensory, modulatory, or motor neurons (9), making it an ideal system to model how serotonin functions in internal states-driven behavioral plasticity.

Widespread mitochondrial injury in nonneural tissues represents a profound change in the internal state. In *C. elegans*, mitochondrial injury and other forms of physiological disruption induce acquired aversion to bacteria for which the worms show innate preference (12). We therefore employ mitochondrial disruption as a way to alter the internal state. Here, we identify a serotonergic circuit that regulates stress-induced aversive learning, which is distinct from the one previously reported to control aversive learning for pathogenic bacteria (13). We map neurons required for the formation and expression of such learned aversive behavior, and document changes in neuronal response property induced by mitochondrial stress. These findings reveal a modulatory serotonergic circuit that connects organismal mitochondrial dysfunction to acquired aversive behavior.

Significance

Physiological stress triggers avoidance behavior, allowing the animals to stay away from potential threats and optimize their chance of survival. Mitochondrial disruption, a common physiological stress in diverse species, induces the nematode *Caenorhabditis elegans* to avoid non-pathogenic bacteria through a serotonergic neuronal circuit. We find that distinct neurons, communicated through serotonin and a specific serotonin receptor, are required for the formation and retrieval of this learned aversive behavior. This learned avoidance behavior is associated with increased serotonin synthesis, altered neuronal response property, and reprogramming of locomotion patterns. The circuit and neuromodulatory mechanisms described here offer important insights for stress-induced avoidance behavior.

Author affiliations: [a]Institute of Molecular Medicine, College of Medicine, National Taiwan University, Taipei, Taiwan 10002; and [b]Center of Precision Medicine, College of Medicine, National Taiwan University, Taipei, Taiwan 10002

Author contributions: Y.-C.C., C.-P.L., and C.-L.P. designed research; Y.-C.C. and C.-P.L. performed research; Y.-C.C., C.-P.L., and C.-L.P. analyzed data; and Y.-C.C. and C.-L.P. wrote the paper.

The authors declare no competing interest.

This article is a PNAS Direct Submission. P.S. is a guest editor invited by the Editorial Board.

[1]Present address: Howard Hughes Medical Institute and Department of Biological Sciences, Columbia University, NY 10027.

[2]To whom correspondence may be addressed. Email: chunliangpan@gmail.com.

This article contains supporting information online at http://www.pnas.org/lookup/suppl/doi:10.1073/pnas.2115533119/-/DCSupplemental.

Published March 7, 2022.

Results

Mitochondrial Disruption Triggers Learned Bacterial Avoidance. Serotonin is involved in learned avoidance of innocuous bacteria in the presence of concomitant disruption of core physiological functions, including mitochondrial respiration (12). We first confirmed that *C. elegans* fed on the OP50 *Escherichia coli* strain for 6 h with Antimycin A, which blocks mitochondrial cytochrome *c* reductase, displayed robust bacterial avoidance, whereas worms grown on control, ethanol-containing OP50 plates rarely left the bacterial lawn (Fig. 1 *A* and *B*). Similar avoidance was observed in *C. elegans* fed on the HT115 *E. coli* strain with RNA interference (RNAi) against genes for mitochondrial functions, such as *atp-2*/ATP synthase and *spg-7*/mitochondrial matrix protease, for 48–56 h until reaching L4 or young D1 (*SI Appendix*, Fig. S1 *A* and *B*). Antimycin A treatment resulted in the fragmentation of mitochondria in the intestine and muscles, while neuronal mitochondria remained morphologically intact (*SI Appendix*, Fig. S1 *C–E*). This indicates that bacterial avoidance is largely the consequence of mitochondrial disruption in nonneural tissues. Consistent with this idea, we found that a transgene that knocks down *fzo-1*, which controls mitochondrial fusion, in neurons did not trigger bacterial avoidance (*SI Appendix*, Fig. S1*F*) (14).

Animals treated with 2.25 μM Antimycin A on OP50 for 3 h displayed significantly stronger avoidance behavior when transferred to a plate seeded with the same bacteria in the absence of Antimycin A, compared to a control bacterial species, HT115 (Fig. 1 *C* and *D*). This confirms that stressed worms avoid the bacteria instead of Antimycin. Using a bacterial chemotaxis assay (Fig. 1*E*), we showed that *C. elegans* retained the acquired bacterial aversion at least for 15 h but not 24 h (Fig. 1*F*), a duration comparable to other forms of long-term memory in this nematode (15, 16). Mitochondria were restored to a largely tubular morphology in the muscles and the intestine 15 h off Antimycin A treatment, suggesting that bacterial aversion is not simply a consequence of persistent mitochondrial injury (*SI Appendix*, Fig. S1 *C* and *D*). Moreover,

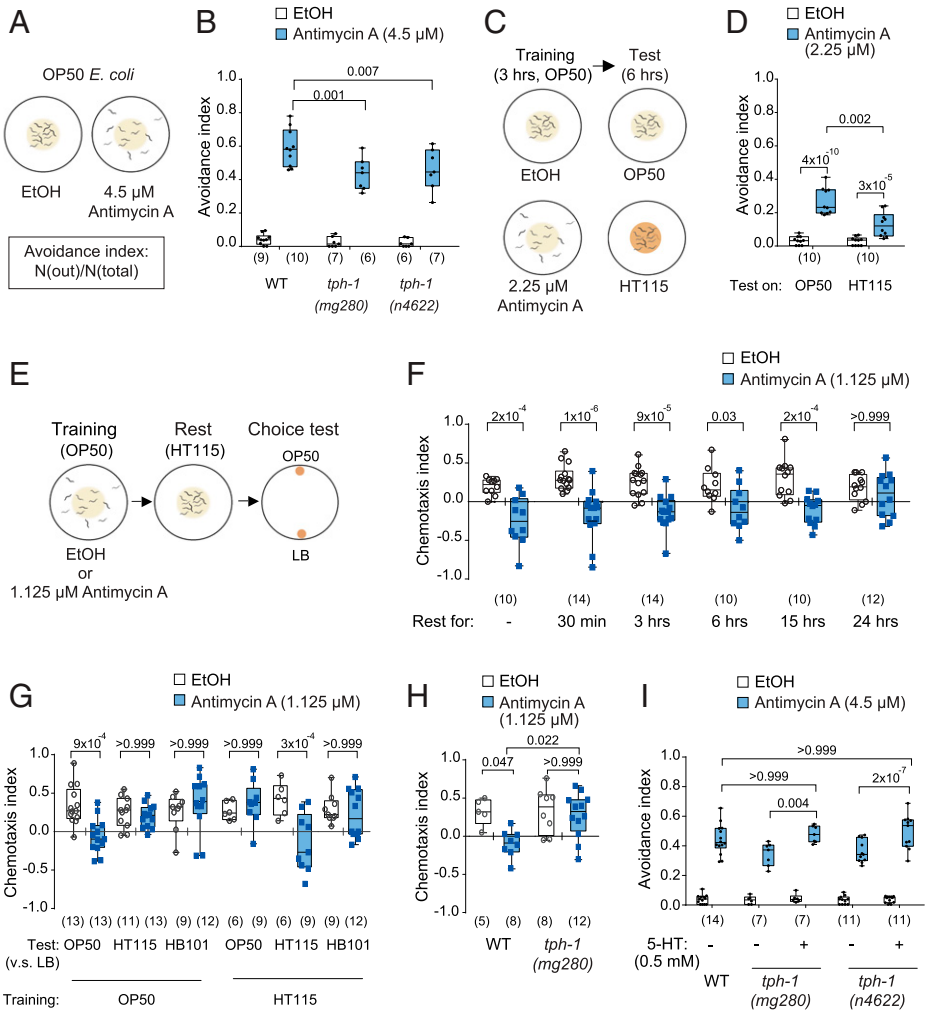

Fig. 1. Serotonin is required for learned bacterial avoidance triggered by mitochondrial disruption. (*A*) Schematic diagram of the avoidance assay using a small bacterial lawn with Antimycin A. (*B*) Quantification of learned bacterial avoidance of the wild type and the two *tph-1* mutant alleles. (*C*) Schematic diagram of the avoidance assay using Antimycin-free bacterial plates. Animals were first trained on OP50 plates with 2.25 μM Antimycin A for 3 h, and were then transferred to OP50 plates without Antimycin A for evaluation of bacterial avoidance six hours later. (*D*) Quantification of bacterial avoidance 6 h after wild-type animals were transferred to Antimycin-free bacterial plates. (*E*) Schematic diagram of the bacterial chemotaxis assay. (*F*) Quantification of bacterial chemotaxis of the wild type with different rest periods. The length of the rest period on HT115 *E. coli* after Antimycin training ranged from 0 to 24 h as indicated. (*G*) Quantification of bacterial chemotaxis of the wild type with matched or mismatched bacterial strains. (*H*) Quantification of bacterial chemotaxis of the *tph-1(mg280)* mutant previously trained on a small bacterial lawn with Antimycin A. (*I*) Quantification of learned bacterial avoidance of two *tph-1* mutant alleles, *mg280* and *n4622* pretreated with 0.5 mM serotonin. Results of individual assays are shown; *n* = numbers of assays, with 50–200 animals per assay. Individual data points with median ± quartiles and 10%/90% whiskers and *P* values are indicated. Two-way ANOVA followed by Bonferroni's correction.

C. elegans showed aversion to the *E. coli* strain on which it was cultured with Antimycin A, while its innate attraction to other *E. coli* strains was unaffected (Fig. 1*G*). These data confirm that bacterial avoidance induced by mitochondrial disruption displays features of long-term associative memory.

Serotonin Regulates Learned Bacterial Avoidance. Consistent with a previous study (12), we found that two null mutations of *tph-1*, which encodes tryptophan hydroxylase for serotonin synthesis (9), impaired learned bacterial avoidance under mitochondrial insults (Fig. 1*B* and *SI Appendix*, Figs. S1*B* and S2*A*). Unlike the wild type, whose innate preference for the OP50 *E. coli* strain was reduced or switched to aversion after Antimycin A treatment, the trained *tph-1* mutants showed defects of aversive learning in the bacterial chemotaxis assay (Fig. 1*H*). Because *tph-1* mutant animals had been reported to display abnormal roaming behavior that could reduce their stay on the bacterial lawn and thus result in less efficient associative learning, we treated *tph-1* mutant animals on a bacterial lawn that covered the entire agar plate, and confirmed that the *tph-1* mutant displayed defective aversive learning (*SI Appendix*, Fig. S2*B*). Innate aversion to nonassociative repulsive odors and locomotion parameters, including speed and reversal, were not significantly different between the wild-type and the *tph-1* mutants (*SI Appendix*, Fig. S2 *C–G*), suggesting that reduced learned bacterial avoidance of the *tph-1* mutant is not a consequence of impaired sensation or locomotion and supporting a specific role of *tph-1* in learned bacterial aversion.

To further confirm the importance of serotonin, we pretreated the *tph-1* mutants with 0.5 mM serotonin for 3 h before testing them for Antimycin A-induced bacterial aversion on serotonin-free plates, which minimizes the effects of serotonin on *C. elegans* locomotion (6, 10). Pretreatment with 0.5 mM serotonin was sufficient to rescue the avoidance defect of the *tph-1* mutants, confirming that serotonin is essential for learned bacterial aversion (Fig. 1*I*). To test whether serotonin enhances learned avoidance under mitochondrial insults, we tested the animals at a much lower concentration, 1.125 μM, of Antimycin A, at which the worms displayed less bacterial avoidance than that under the standard 4.5 μM Antimycin A (*SI Appendix*, Fig. S2*H*). Serotonin significantly enhanced bacterial avoidance at 1.125 μM concentration of Antimycin A but showed no effects in the absence of mitochondrial insults (*SI Appendix*, Fig. S2*H*). These results indicate that serotonin is required for and can enhance learned bacterial avoidance under mitochondrial disruption.

Identification of the Serotonergic Neurons for Learned Avoidance Behavior. We next mapped the serotonergic circuit for learned bacterial aversion under mitochondrial insults. In the *C. elegans* hermaphrodite, there are three pairs of serotonergic neurons: the ADF chemosensory neurons, the NSM modulatory neurons, and the HSN motor neurons that control egg-laying (9, 17, 18). Expression of the *tph-1* genomic DNA in NSM, but not in ADF or HSN, fully restored learned bacterial avoidance under Antimycin A- or RNAi-induced mitochondrial damage (Fig. 2 *A* and *B* *SI Appendix*, Fig. S3 *A–C*). Moreover, NSM-specific overexpression of *tph-1* in the wild type significantly enhanced learned bacterial avoidance at low concentration of Antimycin A (Fig. 2*C*). We conclude that NSMs are the source of serotonin for learned bacterial avoidance under mitochondrial insults.

To investigate whether NSM activation is essential for learned bacterial avoidance, we silenced these neurons by

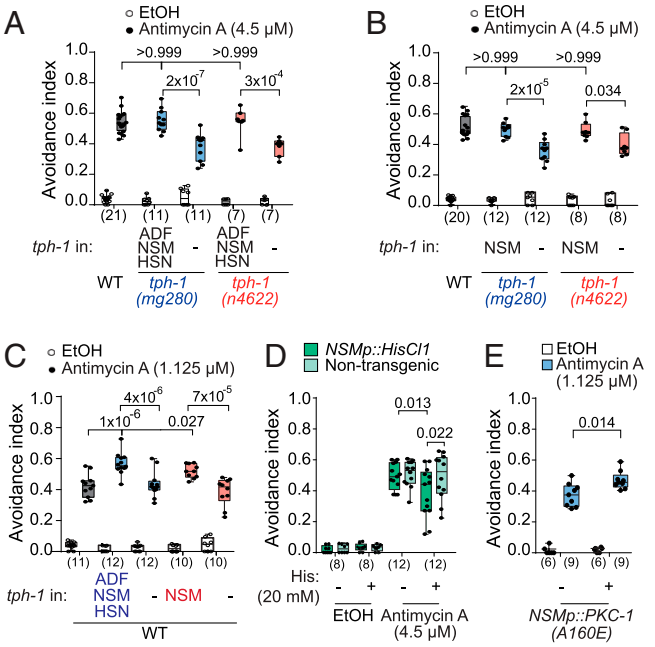

Fig. 2. The serotonergic NSM neurons promote learned bacterial avoidance under mitochondrial stress. (*A* and *B*) Quantification of learned bacterial avoidance of the two *tph-1* mutants expressing genomic *tph-1* in all serotonergic neurons (*A*) or the NSM neurons (*B*). (*C*) Quantification of learned bacterial avoidance of the wild type overexpressing genomic *tph-1* in all serotonergic neurons or the NSM neurons. (*D*) Quantification of learned bacterial avoidance of animals expressing the HisCl1 histamine-gated chloride channel specifically in NSM under the treatment of 20 mM histamine. (*E*) Quantification of learned bacterial avoidance of wild-type animals expressing the gain-of-function PKC-1(A160E) specifically in NSM. Non-transgenic siblings of the *tph-1* mutants (*A–C*) or wild-type animals (*D* and *E*) with the transgenes served as the control genetic background. Worms were treated with indicated concentrations of Antimycin A for 6 h in all the experiments. The results of individual assays are shown; *n* = numbers of assays, with 50–200 animals per assay. Individual data points with median ± quartiles and 10%/90% whiskers and *P* values are indicated. Two-way ANOVA followed by Bonferroni's correction.

histamine-induced hyperpolarization via the *Drosophila* histamine-gated chloride channel 1 (HisCl1) (19). Histamine significantly reduced the learned avoidance behavior of worms that expressed HisCl1 in NSM but not in ADF (Fig. 2*D* and *SI Appendix*, Fig. S3*D*). Therefore, activation of the NSM neurons is required for learned bacterial aversion. We further asked whether NSM synaptic output is sufficient to drive bacterial avoidance under mitochondrial damage. To this end, we expressed PKC-1(A160E) (20), a gain-of-function synaptic protein kinase C that stimulates the release of neurotransmitters and neuromodulators (21), in the NSM neurons. Increased synaptic output from NSM via PKC-1(A160E) expression enhanced learned bacterial avoidance in animals subjected to mild mitochondrial insults without affecting the behavior in naïve animals (Fig. 2*E*). Together, these results indicate that NSM activity is important, and increased NSM synaptic output can enhance learned bacterial avoidance under mitochondrial insults.

Learned Bacterial Avoidance Requires the SER-4 Serotonin Receptor in the RIB Interneurons. To identify neurons that serotonin targets in learned bacterial avoidance, we examined mutants that lack each of the five putative serotonin receptors. The mutants of *ser-1*, *ser-5*, *ser-7*, or *mod-1* displayed intact learned avoidance behavior (Fig. 3*A*). By contrast, the *ser-4* mutant showed reduced learned avoidance (Fig. 3*A* and *SI Appendix*, Fig. S4*A*), and exogenous serotonin failed to restore

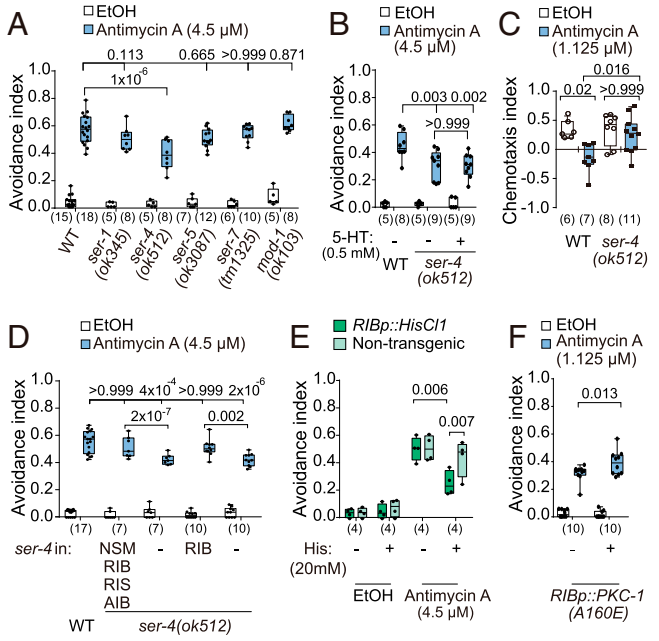

Fig. 3. Learned avoidance behavior requires the SER-4 serotonin receptor in the RIB interneurons. (*A*) Quantification of learned bacterial avoidance in the single mutants for the five putative serotonin receptor genes. (*B*) Quantification of learned bacterial avoidance of *ser-4* pretreated with 0.5 mM serotonin. (*C*) Quantification of bacterial chemotaxis of the *ser-4* mutant. (*D*) Quantification of learned bacterial avoidance of the *ser-4* mutants expressing *ser-4* cDNA in all *ser-4*-expressing neurons or RIB. (*E*) Quantification of learned bacterial avoidance of animals expressing the HisCl1 histamine-gated chloride channel specifically in RIB under treatment of 20 mM histamine. (*F*) Quantification of learned bacterial avoidance in animals expressing gain of function PKC-1(A160E) specifically in RIB. For *D–F*, non-transgenic siblings of the *ser-4* mutant (*D*) or wild-type animals (*E* and *F*) with the transgenes served as the control genetic background. Worms were treated with indicated concentrations of Antimycin A for 6 h (*A, B*, and *D–F*) or 3 h (*C*) in the experiments. The results of individual assays are shown; *n* = numbers of assays, with 50–200 animals per assay. Individual data points with median ± quartiles and 10%/90% whiskers and *P* values are indicated. Two-way ANOVA followed by Bonferroni's correction.

avoidance of the *ser-4* mutant to the wild-type level, suggesting that SER-4 is the receptor that transduces serotonin signal (Fig. 3*B*). Furthermore, we found that the preference of the *ser-4* mutant for OP50 was not altered by Antimycin A (Fig. 3*C* and *SI Appendix*, Fig. S4*B*). Avoidance to the nonassociative repulsive odors and locomotion of the *ser-4* mutant were indistinguishable from that of the wild type (*SI Appendix*, Fig. S4 *C–G*). These results suggest that NSM-derived serotonin acts through the SER-4 receptor to promote learned bacterial avoidance under mitochondrial insults.

With a *ser-4* promoter-mCherry reporter, we confirmed that *ser-4* was expressed in NSM, as well as in several interneurons, including RIB, RIS, and AIB, as reported (22). Expression of *ser-4* cDNA in RIB, but not in NSM, RIS, or AIB, completely restored learned bacterial avoidance of the *ser-4* mutant to the wild-type level (Fig. 3*D* and *SI Appendix*, Fig. S4*H*). These results indicate that serotonin targets the SER-4 receptor in RIB to drive learned bacterial avoidance under mitochondrial insults. To confirm that RIB activation is essential, we silenced RIB by HisCl1-mediated hyperpolarization. Animals expressing HisCl1 in RIB displayed reduced learned bacterial avoidance upon histamine application, while HisCl1 expression alone without histamine did not alter this avoidance behavior, indicating the requirement of RIB activity for learned bacterial aversion (Fig. 3*E*). Moreover, increasing RIB synaptic output via PKC-1(A160E) expression significantly enhanced bacterial avoidance in animals subjected to mild mitochondrial insults (Fig. 3*F*). Together, our results demonstrate that RIB activity is necessary for learned aversion, and enhanced RIB synaptic release promotes bacterial avoidance under mitochondrial stress.

NSM and RIB Regulate the Acquisition and Expression of Learned Aversive Behavior, Respectively. To distinguish the contribution of NSM and RIB in the acquisition (formation) and expression (retrieval) of learned bacterial aversion induced by mitochondrial insults, we silenced individual neuronal classes, via histamine-HisCl1, specifically in the training phase with Antimycin A, or in the testing phase of the bacterial choice assay (Fig. 4*A*). Silencing NSM during the training, but not the testing phase, significantly diminished learned bacterial aversion, suggesting that NSM is important for the acquisition of aversive memory (Fig. 4*B*). By contrast, silencing RIB during training did not prevent the animals from developing aversion for OP50, but RIB inhibition in the testing phase reduced learned bacterial aversion, implicating a role for RIB in the expression of aversive behavior (Fig. 4*C*). These results were confirmed by standard avoidance assays without Antimycin (*SI Appendix*, Fig. S5 *A–C*). Together, these data suggest the acquisition and expression of learned bacterial aversion under mitochondrial insults require distinct neurons of the serotonergic circuit.

Mitochondrial Stress Increases NSM Serotonin Synthesis and Alters RIB Response Property to Bacterial Cues. It is possible that NSM responds to systemic mitochondrial dysfunction by

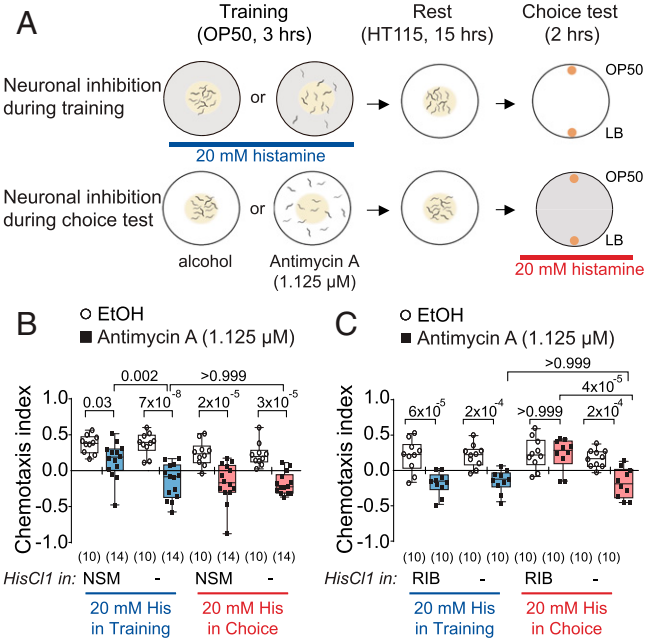

Fig. 4. NSM and RIB differentially regulate the formation and retrieval of learned aversive behavior. (*A*) Schematic diagram of temporally specific inhibition of neurons by 20 mM of histamine during the training phase or the choice test of the OP50 bacterial chemotaxis assay. Animals were trained on a small OP50 bacterial lawn with a resting period of 15 h on the HT115 bacterial strain. (*B* and *C*) Quantification of bacterial chemotaxis of animals expressing the HisCl1 histamine-gated chloride channel specifically in NSM (*B*) or RIB (*C*) under the treatment of 20 mM histamine in either the training or test phase. Nontransgenic siblings of the wild-type animals with the HisCl1 transgenes served as the control genetic background. The results of individual assays are shown; *n* = numbers of assays, with 50–200 animals per assay. Individual data points with median ± quartiles and 10%/90% whiskers and *P* values are indicated. Two-way ANOVA followed by Bonferroni's correction.

increasing serotonin synthesis. To test this, we quantified *tph-1* gene expression using a *tph-1* promoter-GFP reporter. *tph-1* expression began to increase in the NSM cell body 1 h after Antimycin A treatment, and it plateaued after 3 h of Antimycin A treatment or longer, compared to that in the control (Fig. 5 *A* and *B*). By contrast, the expression level of *Ptph-1::GFP* in ADF neurons remained comparable between the naïve and Antimycin A-treated animals (Fig. 5 *C* and *D*). These results suggest that serotonin synthesis in NSM is increased by mitochondrial insults via enhanced *tph-1* transcription. Increased NSM serotonin synthesis early after stress induction is consistent with the role of NSM in the formation of aversive memory.

The minor NSM process was likely a dendrite, with the other two major branches expressing axonal markers (23). Using the synaptic vesicle marker mCherry::RAB-3, which localizes to the cell body and the axonal varicosities that represent presynaptic structures, we confirmed that the two major branches were axons (*SI Appendix*, Fig. S6*A*). A recent study shows that NSM is activated by food ingestion via two acid-sensing ion channel (ASICs) subunits, DEL-3 and DEL-7, that localize to the NSM minor process (24). Learned bacterial avoidance was intact in the *del-3* and *del-7* single mutants as well as in the *del-3; del-7* double mutants, suggesting that these ASIC proteins are not involved in learned bacterial aversion induced by mitochondrial disruption (*SI Appendix*, Fig. S6*B*).

To further explore how mitochondrial stress alters nervous system functions to promote avoidance behavior, we characterized calcium transients of NSM and RIB evoked by OP50 supernatant, using the genetically encoded calcium indicator GCaMP6s (25). NSM in naïve animals did not respond to the OP50 cues. In roughly half of the Antimycin A-treated animals, we documented increased calcium responses in the NSM axon upon removal of the OP50 cues (*SI Appendix*, Fig. S6 C and *D*). However, because our data suggest that the activity of NSM is dispensable during the retrieval of aversive memory (Fig. 4*B*), the implication of this change in NSM response property is unclear. RIB in the majority of animals was insensitive to bacterial cues irrespective of the mitochondrial state (Fig. 5 *E* and *F*). However, in ∼30% of the control animals, RIB showed increase in axonal calcium transients upon stimulation by the OP50 cues (Fig. 5 *E* and *F*). In a fraction (∼25%) of the Antimycin A-treated animals, we recorded robust calcium transients in the RIB axon upon removal of the OP50

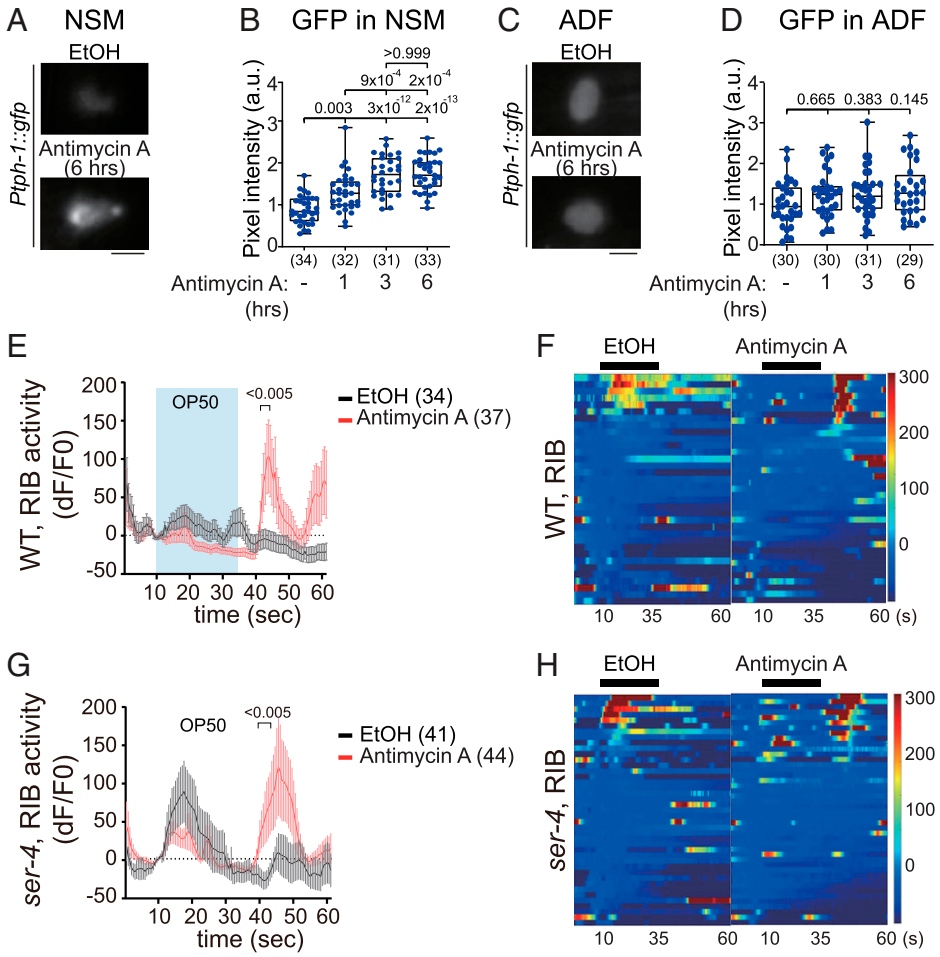

Fig. 5. Mitochondrial stress increases NSM serotonin synthesis and alters RIB response property. (*A* and *B*) Epifluorescent images (*A*) and quantification of GFP level (*B*) in NSM at different time points after 4.5 μM Antimycin A treatment. (*C* and *D*) Epifluorescent images (*C*) and quantification of GFP level (*D*) in ADF at different time points after Antimycin A treatment. In (*A–D*), GFP was from the integrated transgene *mgIs42(Ptph-1::GFP)*. Worms were treated with 4.5 μM Antimycin A for indicated time (*B* and *D*). The results of measurement of individual cells are shown; *n* = numbers of cells. Individual data points with median ± quartiles and 10%/90% whiskers and *P* values are indicated. One-way ANOVA with Bonferroni corrections (*B* and *D*). Scale bar = 5 μm. (*E* and *F*) Average GCaMP6s signal intensity (*E*) and heat map presentation of GCaMP6s signal (*F*) in the RIB axon of the naive and trained wild-type animals. (*G* and *H*) Average (*G*) and heat map presentation (*H*) of axonal GCaMP6s signals in the RIB axon of naive and Antimycin A-treated *ser-4* mutants. In (*F*) and (*H*), the black bars indicate stimulation with the OP50 supernatant, with the *x*-axis for individual neurons and *y* axis for time scale. Animals were treated with 4.5 μM Antimycin A for 6 h. Data are mean ± standard error of mean (SEM). *P* values are indicated. Multiple *t* tests.

cues, which was absent in the control animals (Fig. 5 *E* and *F*). To test whether these changes in RIB response property requires serotonin signaling, we examined RIB activity in the *ser-4* mutant. Neither ON- nor OFF-responses of the RIB axon to the OP50 supernatant were discernibly altered in the *ser-4* mutant treated with Antimycin A (Fig. 5 *G* and *H*). These findings raise the possibility that serotonin signaling modulates RIB downstream of membrane excitation, such as signal transduction or presynaptic functions, which could not be evaluated by calcium imaging.

Serotonergic Signaling Shapes *C. elegans* Behavioral Strategies to Promote Learned Bacterial Avoidance. We have mapped a serotonergic circuit with defined neurons, signals and receptors essential for learned bacterial aversion under mitochondrial insults. To understand how these genetic and cellular factors regulate avoidance behavior, we sought to determine elementary behavioral components that collectively reprogram worm locomotion to drive bacterial avoidance. High-angle turn (pirouette) is a key locomotion strategy that modulates chemotaxis behavior in *C. elegans* (26). Worms decrease the frequency of pirouettes when moving up the gradient of attractive cues, and increase pirouette frequency when moving down the attractant gradient (26). The relationship between sensory cue concentration and pirouette frequency is reversed in aversive chemotaxis (21).

We first analyzed the correlation between pirouette frequency and the alignment of worm movement with the bacterial sensory cues defined by the bearing angle (Fig. 6*A*). Bearing angles less than 90° suggest that worms are moving toward the bacteria, whereas bearing angles between 90° and 180° suggest that worms are moving away from the bacteria. In control wild-type animals, the pirouette frequency as a function of bearing angles was consistent with a typical attractive response (Fig. 6*B*). Antimycin A treatment altered the bearing angle-pirouette function to become a typical avoidance response (Fig. 6*B*). These data suggest that pirouette frequency in response to sensory signals is a key regulatory target of mitochondrial stress in learned avoidance behavior. The *tph-1* and *ser-4* mutations

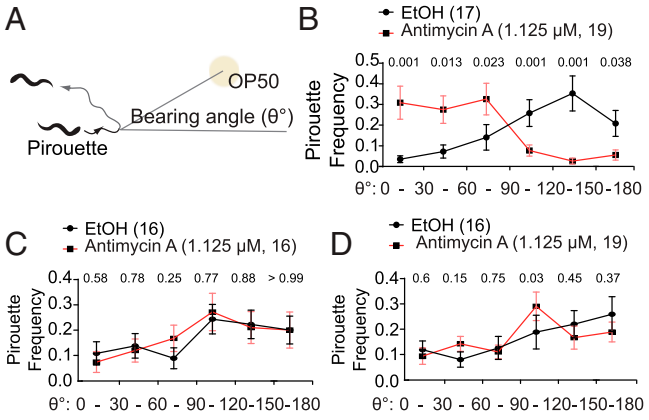

Fig. 6. Serotonin promotes bacterial avoidance by modulating the bias of turning frequency to bacterial cues. (*A*) Schematic diagram of pirouette and bearing angles (*θ*), which measures the alignment between the moving direction of the animal with that toward the OP50 cue. Pirouettes are reversals followed immediately by an omega turn. (*B–D*) Quantification of pirouette frequency as a function of bearing angles of the wild-type (*B*), *tph-1* (*C*), and *ser-4* mutants (*D*) over a 10-min and 20-min duration for the control (EtOH) and Antimycin A-treated strains. The bearing angles are binned at 30°. The turning frequencies are normalized against the total numbers of turns in each genotype-condition group. Animals were treated with 1.125 μM Antimycin A for 3 h. N are the numbers of recorded animals. Bars are mean ± SEM. *P* values are indicated. Multiple *t* tests.

abolished the effects of mitochondrial stress on pirouette frequency (Fig. 6 *C* and *D*). These data suggest that serotonin signaling modulates pirouette as a critical locomotion strategy to promote learned bacterial avoidance under mitochondrial insults.

Discussion

In this study, we find that a *C. elegans* neural circuit translates organismal-wide mitochondrial stress to serotonergic signals, which may alter behavioral strategies and enable associative aversive behavior. This circuit is composed of the NSM neuron, which secrets serotonin and acts in memory formation, and the RIB interneuron, which receives the serotonin signal and retrieves aversive memory. In a fraction of animals, the RIB develops distinct sensory-evoked responses after the animal is primed by mitochondrial stress, suggesting that in these cases, RIB may act as a hub that connects internal states and behavioral outputs. These findings offer mechanistic insights into stress-induced behavioral plasticity.

Aversive Learning and Behavior Induced by Physiological Stress. Physiological stress can profoundly influence animal behavior. It is important that animals learn to recognize sensory cues associated with increased physiological stress and develop behavioral adaptation to minimize future encounter with these cues. *C. elegans* learns to avoid the pathogenic bacteria *Pseudomonas aeruginosa*, as infection by *Pseudomonas* drives aversive associative learning to avoid this pathogen (13, 27–30). Microbial toxins and metabolites often target mitochondria in the host (31). In the current study, we adapt mitochondrial dysfunction as a trigger for aversive learning of bacterial cues that are otherwise attractive for *C. elegans* in the absence of mitochondrial disruption. This paradigm is conceptually similar to conditioning in mammals. However, in contrast to classical Pavlovian conditioning, in which the conditioned stimulus is usually neutral, our model shows that the positive valence of an innate attractive cue (*E. coli*) can be altered by pairing it with mitochondrial stress to become negative. The relative simplicity of the nervous system and the ease to manipulate internal states make invertebrates such as *C. elegans* a powerful model to study stress-induced behavioral plasticity. It will be important to conduct similar studies in mammals to understand to which extent the mechanisms for stress-induced aversive learning are conserved in both invertebrates and vertebrates.

Serotonergic Modulation and Stress-Induced Aversive Learning. Serotonin regulates various aspects of aversive learning, including the formation and retrieval of aversive memory (32), adaptive olfactory aversion associated with starvation (33) and anticipation of aversive signals (34). In *C. elegans*, serotonin is involved in regulating the sensitivity to the repulsive odor, 1-octanol, depending on the feeding status of the animal (34). Melo and Ruvkun had shown that serotonin is required for learned bacterial avoidance under mitochondrial stress (12). We confirm this finding and show that the NSM modulatory neuron responds to systemic mitochondrial dysfunction by producing serotonin, and it acts in the establishment of learned bacterial aversion. By contrast, the RIB interneuron receives NSM-derived serotonin through the SER-4 receptor and acts to express the aversive behavior. This two-tier circuit for aversive learning is reminiscent of a recently identified *C. elegans* circuit for olfactory imprinting, in which tyramine connects neurons for the formation and retrieval of aversive imprinted memory, respectively (35). Because NSM and RIB do not form

direct synaptic contact, serotonin likely acts extrasynaptically as a neuromodulator, and could target neurons other than RIB.

Early increase of *tph-1* transcription in NSM after the induction of mitochondrial stress suggests that the NSM neuron may monitor and encode the internal states of mitochondrial dysfunction through serotonin synthesis. NSM is known to mediate the effects of feeding status on *C. elegans* foraging behaviors (11, 24). These observations, together with those in the current study, raise the intriguing possibility that NSM functions as an interoceptive neuron akin to those in the mammalian hypothalamus (36). The minor process of NSM has molecular markers of a dendrite and expresses two ASIC (acid-sensing ion channel) subunits, DEL-3 and DEL-7, that are required for detecting food cues during foraging behavior (24). However, we find that *del-3* and *del-7* are not required for bacterial aversion induced by mitochondrial stress. This suggests that unknown sensory molecules other than ASICs in the NSM dendrite are responsible for detecting internal state changes and promote serotonin synthesis in NSM. Alternatively, in stress-conditioned animals, NSM may respond to external cues indirectly via other sensory neurons. This view is supported by our finding that bacterial cues evoke OFF-responses in the NSM axons of many Antimycin-treated, but not the naïve animals.

Rhoades et al. reported NSM ON-responses in freely moving, starved worms shortly after their entry into the bacterial lawn, although it is not clear whether the NSM responses were recorded from the soma or the processes (24). In fed animals, NSM showed little responses to food encounter within the same time window. Similarly, we detected no such ON-responses to bacterial cues in well-fed wild-type animals without mitochondrial stress. In our study, NSM responses were evoked by bacterial chemosensory cues in stressed animals. In Rhoades et al., it was hypothesized that NSM responded to food ingestion as well as the mechanical stimulation that accompanies food ingestion (24). NSM responses were obtained in freely moving animals in the prior study, while in the current study, we recorded NSM calcium dynamics from animals immobilized in a microfluidic chip. These differences suggest that NSM responses depend on the states of the animal as well as the sensory stimuli applied to this neuron. Nevertheless, as inhibition of NSM activity during memory retrieval does not disrupt the avoidance behavior, the significance and implication of this stress-induced NSM OFF-response remain elusive.

Serotonergic Signaling Reprograms Behavioral Strategy to Induce Learned Aversion. In contrast to NSM, the RIB interneuron functions in expressing the learned bacterial avoidance. RIB regulates olfactory sensory behaviors (37), but it remains unknown how RIB responds to sensory cues, or which specific locomotion elements it regulates in diverse behavioral contexts. Naïve *C. elegans* decreases the pirouette frequency as it approaches the attractive odors (26). By contrast, Antimycin A induces high frequency of pirouette when the animal approaches OP50, which requires *ser-4*. These data imply that serotonin signaling facilitates bacterial avoidance by altering the odor-pirouette frequency function, likely through RIB. In a fraction of naïve animals, the RIB axon responds to the OP50 cues, which could be explained by direct synaptic connection of RIB to several sensory neurons (38). Similar to the case of NSM, Antimycin induces OFF-responses upon the removal of OP50 cues in some animals. The *ser-4* mutation does not alter RIB OFF-responses. This suggests that serotonin signaling may act downstream of RIB membrane excitability, such as in the signal transduction process or presynaptic functions. OFF-responses are widely employed in diverse neuronal types for information encoding or processing, such as the photoreceptors and certain bipolar cells in the mammalian retina, the L2 pathway neurons for motion detection in the *Drosophila* optic lobe (39), and the *C. elegans* AWC olfactory neurons (40). The molecular basis of stress-induced OFF-responses in NSM and RIB remains unknown. It should be noted that in a significant fraction of animals, both NSM and RIB remain insensitive to bacterial cues irrespective of the mitochondrial state, suggesting that they may respond to other unidentified sensory stimuli. Further studies are necessary to uncover genes that shape response properties under mitochondrial stress in NSM and RIB.

Materials and Methods

***C. elegans* and *E. coli* Bacterial Strains.** *C. elegans* strains were cultured and maintained as previously described (41). Briefly, animals are cultured on solid nematode growth medium (NGM) seeded with *E. coli* OP50 as food at 20 °C unless specified otherwise. Care is taken to avoid overcrowding or starvation. The HT115 *E. coli* strains were used in indicated experiments. A list of mutant alleles and transgenic strains used in this study is available in *SI Appendix*, Table S1.

Molecular Biology and Germline Transformation. Standard molecular biology techniques were used in this study. Promoter sequences used included *tph-1* (2.8 kb), *tph-1* short (*tph-1s*, 158 bp, for NSM-specific expression), *srh-142* (3.4 kb, for ADF-specific expression), *unc-86* (5 kb, for HSN expression), *ser-4* (5 kb), *sto-3* (1 kb, for RIB expression), *npr-9* (2 kb, for AIB expression), and *flp-11* (2.5 kb, for RIS expression), which were cloned into pPD95.75 or pPD95.77 vectors. The genomic *tph-1* sequence (2.4 kb) and the cDNA of *ser-4* (1.3 kb) were used in the rescue experiments. Transgenic animals were generated by microinjection-based germline transformation as described (42). Briefly, purified DNA of constructs of interest at defined concentrations was mixed immediately before loading into a glass micropipette. Young adult hermaphrodites that contain less than five embryos are used for injection.

Avoidance Assay with Antimycin A. Two to four adult gravid hermaphrodites were allowed to lay eggs overnight. The adults were then removed and hatched larvae on the plate were reared to day one young adult (D1). One hundred microliters of OP50 in LB (optical density [OD] = 0.4–0.6) was seeded at the center of the NGM plate to make a lawn of defined area the day before the avoidance assay. Antimycin A (Sigma-Aldrich) from the stock (2.5 mg/mL, in 99% EtOH) was diluted by 1:10 ratio with M9 buffer (0.25 mg/mL), and 100 μl of this Antimycin A dilution was gently and evenly applied onto the bacteria lawn to reach the final concentration of 4.5 μM (2.5 μg/mL) in plate. Plates with lower concentrations of Antimycin A were prepared similarly with adjusted amount of Antimycin A. In the control group, 99% ethanol (EtOH) was used in the place of the Antimycin A stock. After the bacterial plate was completely dried in air, D1 animals were collected and cleaned by washing with M9. Worms were then gently transferred to the center of the assay plates in as little liquid as possible. Bacterial avoidance was scored 6 h later or as indicated in individual experiments by the avoidance index, which is the fraction of worms staying outside the OP50 lawn: N_{out}/N_{total}, where N_{out} is the number of worms off-lawn and N_{total} is the number of total worms on the plate. In experiments where Antimycin-treated animals were transferred to an Antimycin-free plate for avoidance assay, animals were first treated with 2.25 μM of Antimycin A for 3 h on a small or full bacterial lawn as indicated in specific experiments and were transferred by washing with M9 to an NGM plate seeded with 100 μl of OP50 or HT115 *E. coli* without Antimycin A. The avoidance index was quantified 6 h after the transfer.

Avoidance Assay with RNAi. RNAi avoidance assays were performed as described with some modifications (12). In brief, overnight-grown *atp-2, spg-7*, and control (L4440) RNAi bacterial culture was diluted at 1:100 ratio and grown for 3 h (OD = 0.4–0.6), followed by 1 mM isopropyl β-D-1-thiogalactopyranoside (IPTG) induction for 1 h. A total of 100 μl of HT115 was dropped to the center of the NGM plate and was kept at room temperature overnight to allow IPTG to induce double-stranded RNA. On the next day, hatched L1 larvae were transferred to the center of the assay plates. Lawn leaving was scored 48–56 h later. Avoidance index was calculated as described.

Bacterial Chemotaxis Assay. Bacterial chemotaxis assays were performed as described with some modifications (43). The 5.5-cm chemotaxis (CTX) plate (2% agar, 5 mM potassium phosphate [pH 6.0], 1 mM $CaCl_2$, 1 mM $MgSO_4$) was divided into six equal longitudinal zones similar to that used for repulsive chemotaxis assays (44). One microliter of liquid OP50 (OD = 0.4–0.6) and 1 μl of LB were spotted at the opposite sides of the plate, respectively. When these were completely dried, 1 μl of 0.5 M sodium azide was applied to both spots to immobilize the worms that were attracted to reach OP50 or LB. D1 animals were treated with either ethanol or 1.125 μM Antimycin (0.625 μg/mL) on small or full bacterial lawns as indicated in individual experiments for 3 h. This concentration of Antimycin A was used because the standard 4.5 μM of Antimycin A seemed to interfere with worm movements in the bacterial chemotaxis assay. Worms were then collected by washing with M9 for three times and transferred to NGM plates seeded with 200 μL HT115 *E. coli* for 15 h or as specified in individual experiments. The animals were then collected and washed, twice with the CTX wash buffer (5 mM potassium phosphate [pH 6.0], 1 mM $CaCl_2$, 1 mM $MgSO_4$) and once by water. Animals were transferred to the center of the chemotaxis plate and excessive liquid carefully removed by Kimwipes. Two hours later, the chemotaxis index (CI) was quantified as

$$CI = (N_{OP50} - N_{LB})/(N_{OP50} + N_{LB})$$

where N_{OP50} is the number of animals in the two zones close to OP50, and N_{LB} is the number of animals in the two zones close to LB.

Chemotaxis Assays for Repulsive Odors. Chemotaxis assays for 2-nonanone and 1-octanol were performed as described with some modifications (44). The 9-cm chemotaxis (CTX) plate (2% agar, 5 mM potassium phosphate [pH 6.0], 1 mM $CaCl_2$, 1 mM $MgSO_4$) was divided into six equal longitudinal zones similar to that used for repulsive chemotaxis assays (44). One microliter each of ethanol control and undiluted 1-octanol or 2-nonanone at 1:10 dilution (in ethanol) was spotted at the opposite sides of the plate, respectively. When these were completely dried, 1 μL of 0.5 M sodium azide was applied to both spots to immobilize the worms that moved toward either spot. Young D1 animals were then collected and washed, twice with the CTX wash buffer (5 mM potassium phosphate [pH 6.0], 1 mM $CaCl_2$, 1 mM $MgSO_4$) and once by water. Animals were transferred to the center of the chemotaxis plate and excessive liquid carefully removed by Kimwipes. One hour later, the chemotaxis index (CI) was quantified as

$$CI = (N_{odor} - N_{EtOH})/(N_{total})$$

where N_{odor} is the number of animals in the two zones close to either repulsive odor, and N_{EtOH} is the number of animals in the two zones close to the ethanol control. A negative CI indicates aversion to the test odor.

Serotonin Treatment. A serotonin (Sigma-Aldrich) stock solution of 0.5 M was made with distilled water and filtered. Ten microliters of serotonin stock solution were added to the NGM plate to reach a final concentration of 0.5 mM. For control, 10 μL of distilled water were used in the place of serotonin. D1 animals were transferred onto serotonin or control plates seeded with OP50 and cultivated for 3 h. Animals were then washed and transferred to Antimycin A-containing OP50 plates, and the avoidance index was quantified 6 h later.

Histamine Treatment. We performed histamine treatment following a published method with minor modifications (19). In brief, a stock of 2 M histamine dihydrochloride (Sigma-Aldrich) was made with distilled water, pH-adjusted to a final value of 6.3 with 10 N NaOH and filtered. One hundred microliters of the 2 M histamine stock solution were added to the NGM or chemotaxis (CTX) plates to reach the final concentration of 20 mM. The same amount of water was added in place of histamine to the NGM or CTX plates as control. The histamine-containing plates should be stored at 4 °C and used within 1 wk.

Epifluorescent and Confocal Microscopy. To analyze the expression level of *Ptph-1::mCherry* in the cell body of serotonergic neurons, D1 hermaphrodites were immobilized in 1% sodium azide on 5% agar pad and epifluorescent images were acquired by the AxioImager M2 system (Carl Zeiss). The pixel intensity of mCherry was quantified by ImageJ with subtraction of background signals. To examine the mitochondrial morphology in the intestine and body wall muscles, D1 animals carrying *zcIs14(Pmyo-3::GFP^{mt})* and animals carrying *zcIs17(Pges-1:: GFP^{mt})* were treated with ethanol (control) or 4.5 μM Antimcyin A for 6 h. To examine mitochondrial morphology in NSM neurons, D1 animals carrying *twnEx609(Ptph-1s::tomm20::mCherry); twnEx605(Ptph-1s::ds-atp-2)* were immobilized with 1 mM levamisole. Confocal projection images were acquired using the LSM700 Confocal Imaging System (Carl Zeiss).

Calcium Imaging with Microfluidic Device. Calcium imaging using the microfluidic chip was performed as previously described with minor modifications (45). Briefly, young adult worms without or with Antimycin A treatment (4.5 μM, 6 h) were transferred into an olfactory chip (MicroKosmos, Ann Arbor, MI). NGM buffer (25 mM potassium phosphate [pH 6.0], 1 mM $CaCl_2$, 1 mM $MgSO_4$) or OP50 supernatant (OD = 0.5–0.6) was delivered through the VC-8 Valve Control System (Warner Instruments, Holliston, MA) with journals written in MetaMorph (Molecular Devices, San Jose, CA). Fluorescent images were acquired using the ORCA3 sCMOS CCD camera (Hamamatsu Photonics, Japan) and pE-300 LED (CoolLED, UK) at the speed of 2 frames/s and an exposure time of 400 ms at 5% illumination intensity.

Locomotion Assessment. To quantify worm locomotion, three to five well-fed D1 worms were picked to an unseeded plate for crawling for 2 min to shed the bacteria, and they were transferred again to another unseeded plate, with locomotion recorded for three minutes using WormLab (MBF Bioscience, VT). Locomotion parameters analyzed include movement speed, reversal frequency and the fraction of time in forward or backward movement.

Analysis of Pirouette Frequency as a Function of Bearing Angle. To quantify worm pirouette frequency, five to eight D1 worms with or without Antimycin A treatment (1.125 μM, 3 h) were picked to an unseeded plate for crawling for 2 min to shed the bacteria. The worms were transferred again to a CTX plate spotted with 1 μL OP50 (OD = 0.4–0.6) and 1 μl of LB at opposite sides of the plate, respectively. Worm movements were recorded using WormLab for 10 min (control) and 20 min (Antimycin A-treated), respectively. The pirouettes were identified using WormLab, which defines the pirouette as a reversal followed immediately by an omega turn. The bearing angle was defined as the deviation of the movement direction of the worm with respect to the OP50 source.

Statistical Analysis. Statistical analyses, including two-way ANOVA followed by Bonferroni's correction for multiple comparisons, multiple *t* test, Mann-Whitney *U* test and χ^2 test, were performed by Prism and described in the figure legends that apply, with sample sizes indicated.

Data Availability. All study data are included in the article and/or supporting information.

ACKNOWLEDGMENTS. We thank Cori Bargmann, Steven Flavell, Michael Koelle, Chan-Yen Ou, and Yi-Chun Wu for reagents, protocols, and *C. elegans* or bacterial strains, and Llian Mabardi and Yuichi Iino for advice on calcium imaging using the olfactory chip. We thank Yuki Tsukada, Chun-Hao Chen, and the Pan lab members for comments on the manuscript. Some of the strains used in this study are provided by the *Caenorhabditis* Genetics Center, which is supported by NIH Office of Research Infrastructure Programs (P40OD010440), and by the National BioResources Project (NBRP), which is supported by the Japanese government. This study was funded by the Ministry of Science and Technology, and the Featured Areas Research Center Program within the framework of the Higher Education Sprout Project by the Ministry of Education (MOE), Taiwan, to C.-L.P. (MOE 110L901402A, MOST 110-2634-F-002-044, 107-2320-B-002-055-MY3, and 109-2320-B-002-019-MY3).

1. S. M. Sternson, Hypothalamic survival circuits: Blueprints for purposive behaviors. *Neuron* **77**, 810–824 (2013).
2. D. D. Ghosh *et al.*, Neural architecture of hunger-dependent multisensory decision making in *C. elegans*. *Neuron* **92**, 1049–1062 (2016).
3. J. M. Kobler, F. J. Rodriguez Jimenez, I. Petcu, I. C. Grunwald Kadow, Immune receptor signaling and the mushroom body mediate post-ingestion pathogen avoidance. *Curr. Biol.* **30**, 4693–4709.e3 (2020).
4. B. W. Okaty, K. G. Commons, S. M. Dymecki, Embracing diversity in the 5-HT neuronal system. *Nat. Rev. Neurosci.* **20**, 397–424 (2019).
5. Z. Liu *et al.*, Dorsal raphe neurons signal reward through 5-HT and glutamate. *Neuron* **81**, 1360–1374 (2014).
6. H. R. Horvitz, M. Chalfie, C. Trent, J. E. Sulston, P. D. Evans, Serotonin and octopamine in the nematode Caenorhabditis elegans. *Science* **216**, 1012–1014 (1982).
7. L. Ségalat, D. A. Elkes, J. M. Kaplan, Modulation of serotonin-controlled behaviors by Go in Caenorhabditis elegans. *Science* **267**, 1648–1651 (1995).

8. L. E. Waggoner, G. T. Zhou, R. W. Schafer, W. R. Schafer, Control of alternative behavioral states by serotonin in Caenorhabditis elegans. *Neuron* **21**, 203–214 (1998).
9. J. Y. Sze, M. Victor, C. Loer, Y. Shi, G. Ruvkun, Food and metabolic signalling defects in a Caenorhabditis elegans serotonin-synthesis mutant. *Nature* **403**, 560–564 (2000).
10. E. R. Sawin, R. Ranganathan, H. R. Horvitz, C. elegans locomotory rate is modulated by the environment through a dopaminergic pathway and by experience through a serotonergic pathway. *Neuron* **26**, 619–631 (2000).
11. S. W. Flavell *et al.*, Serotonin and the neuropeptide PDF initiate and extend opposing behavioral states in C. elegans. *Cell* **154**, 1023–1035 (2013).
12. J. A. Melo, G. Ruvkun, Inactivation of conserved C. elegans genes engages pathogen- and xenobiotic-associated defenses. *Cell* **149**, 452–466 (2012).
13. Y. Zhang, H. Lu, C. I. Bargmann, Pathogenic bacteria induce aversive olfactory learning in Caenorhabditis elegans. *Nature* **438**, 179–184 (2005).
14. L. T. Chen *et al.*, Neuronal mitochondrial dynamics coordinate systemic mitochondrial morphology and stress response to confer pathogen resistance in *C. elegans*. *Dev Cell* **56**, 1770–1785 e1712 (2021).
15. A. L. Kauffman, J. M. Ashraf, M. R. Corces-Zimmerman, J. N. Landis, C. T. Murphy, Insulin signaling and dietary restriction differentially influence the decline of learning and memory with age. *PLoS Biol.* **8**, e1000372 (2010).
16. C. H. Rankin, C. D. Beck, C. M. Chiba, *Caenorhabditis elegans*: A new model system for the study of learning and memory. *Behav. Brain Res.* **37**, 89–92 (1990).
17. C. Desai, G. Garriga, S. L. McIntire, H. R. Horvitz, A genetic pathway for the development of the Caenorhabditis elegans HSN motor neurons. *Nature* **336**, 638–646 (1988).
18. J. S. Duerr *et al.*, The cat-1 gene of *Caenorhabditis elegans* encodes a vesicular monoamine transporter required for specific monoamine-dependent behaviors. *J. Neurosci.* **19**, 72–84 (1999).
19. N. Pokala, Q. Liu, A. Gordus, C. I. Bargmann, Inducible and titratable silencing of *Caenorhabditis elegans* neurons in vivo with histamine-gated chloride channels. *Proc. Natl. Acad. Sci. U.S.A.* **111**, 2770–2775 (2014).
20. L. V. Dekker, P. McIntyre, P. J. Parker, Mutagenesis of the regulatory domain of rat protein kinase C-eta. A molecular basis for restricted histone kinase activity. *J. Biol. Chem.* **268**, 19498–19504 (1993).
21. M. Tsunozaki, S. H. Chalasani, C. I. Bargmann, A behavioral switch: cGMP and PKC signaling in olfactory neurons reverses odor preference in *C. elegans*. *Neuron* **59**, 959–971 (2008).
22. G. Gürel, M. A. Gustafson, J. S. Pepper, H. R. Horvitz, M. R. Koelle, Receptors and other signaling proteins required for serotonin control of locomotion in *Caenorhabditis elegans*. *Genetics* **192**, 1359–1371 (2012).
23. J. L. Rhoades *et al.*, ASICs mediate food responses in an enteric serotonergic neuron that controls foraging behaviors. *Cell* **176**, 85–97.e14 (2019).
24. C. E. Rhoades *et al.*, Unusual physiological properties of smooth monostratified ganglion cell types in primate retina. *Neuron* **103**, 658–672.e6 (2019).
25. T. W. Chen *et al.*, Ultrasensitive fluorescent proteins for imaging neuronal activity. *Nature* **499**, 295–300 (2013).
26. J. T. Pierce-Shimomura, T. M. Morse, S. R. Lockery, The fundamental role of pirouettes in *Caenorhabditis elegans* chemotaxis. *J. Neurosci.* **19**, 9557–9569 (1999).
27. Y. Liu, B. S. Samuel, P. C. Breen, G. Ruvkun, *Caenorhabditis elegans* pathways that surveil and defend mitochondria. *Nature* **508**, 406–410 (2014).
28. N. V. Kirienko, F. M. Ausubel, G. Ruvkun, Mitophagy confers resistance to siderophore-mediated killing by *Pseudomonas aeruginosa*. *Proc. Natl. Acad. Sci. U.S.A.* **112**, 1821–1826 (2015).
29. M. W. Pellegrino *et al.*, Mitochondrial UPR-regulated innate immunity provides resistance to pathogen infection. *Nature* **516**, 414–417 (2014).
30. H. I. Ha *et al.*, Functional organization of a neural network for aversive olfactory learning in Caenorhabditis elegans. *Neuron* **68**, 1173–1186 (2010).
31. J. H. Jiang, J. Tong, K. Gabriel, Hijacking mitochondria: Bacterial toxins that modulate mitochondrial function. *IUBMB Life* **64**, 397–401 (2012).
32. A. Sengupta, A. Holmes, A discrete dorsal raphe to basal amygdala 5-HT circuit calibrates aversive memory. *Neuron* **103**, 489–505.e7 (2019).
33. M. Fadda *et al.*, NPY/NPF-related neuropeptide FLP-34 signals from serotonergic neurons to modulate aversive olfactory learning in *Caenorhabditis elegans*. *J. Neurosci.* **40**, 6018–6034 (2020).
34. R. Amo *et al.*, The habenulo-raphe serotonergic circuit encodes an aversive expectation value essential for adaptive active avoidance of danger. *Neuron* **84**, 1034–1048 (2014).
35. X. Jin, N. Pokala, C. I. Bargmann, Distinct circuits for the formation and retrieval of an imprinted olfactory memory. *Cell* **164**, 632–643 (2016).
36. S. M. Sternson, Exploring internal state-coding across the rodent brain. *Curr. Opin. Neurobiol.* **65**, 20–26 (2020).
37. E. L. Tsalik, O. Hobert, Functional mapping of neurons that control locomotory behavior in Caenorhabditis elegans. *J. Neurobiol.* **56**, 178–197 (2003).
38. J. G. White, E. Southgate, J. N. Thomson, S. Brenner, The structure of the nervous system of the nematode Caenorhabditis elegans. *Philos. Trans. R. Soc. Lond. B Biol. Sci.* **314**, 1–340 (1986).
39. M. Joesch, B. Schnell, S. V. Raghu, D. F. Reiff, A. Borst, ON and OFF pathways in Drosophila motion vision. *Nature* **468**, 300–304 (2010).
40. S. H. Chalasani *et al.*, Dissecting a circuit for olfactory behaviour in Caenorhabditis elegans. *Nature* **450**, 63–70 (2007).
41. S. Brenner, The genetics of *Caenorhabditis elegans*. *Genetics* **77**, 71–94 (1974).
42. C. C. Mello, J. M. Kramer, D. Stinchcomb, V. Ambros, Efficient gene transfer in *C. elegans*: Extrachromosomal maintenance and integration of transforming sequences. *EMBO J.* **10**, 3959–3970 (1991).
43. C. I. Bargmann, E. Hartwieg, H. R. Horvitz, Odorant-selective genes and neurons mediate olfaction in *C. elegans*. *Cell* **74**, 515–527 (1993).
44. E. R. Troemel, B. E. Kimmel, C. I. Bargmann, Reprogramming chemotaxis responses: Sensory neurons define olfactory preferences in *C. elegans*. *Cell* **91**, 161–169 (1997).
45. N. Chronis, M. Zimmer, C. I. Bargmann, Microfluidics for in vivo imaging of neuronal and behavioral activity in *Caenorhabditis elegans*. *Nat. Methods* **4**, 727–731 (2007).